

# Numerical Analysis of Superconducting Microstrips using Python

Reema Jose  
Department of Physics  
Carmel College Mala  
Thrissur District, Kerala

**Abstract:** The microwave characteristics of high temperature superconducting thin films with the value of the parameter  $\gamma = 4$  and  $\gamma = 2$  are studied using the Coffey-Clem model. Numerical analysis of transmission and reflection coefficients is done by varying the field and temperature. We compared transmission and reflection coefficient of high temperature superconducting films with the value of the parameter  $\gamma = 4$  and  $\gamma = 2$ . The python programming language is employed for the numerical analysis purpose.

**Keywords:-** Superconducting Microstrips, Python program, Transmission Coefficient, Reflection Coefficient.

## I. INTRODUCTION

The study on the propagation characteristics of a superconducting transmission line is widely reported in literature, help us to see the efficiency of the micro strip line in carrying the wave. Many attempts were made to model the complex conductivity of the type 2 superconducting materials as a function of temperature, magnetic field and other material parameters. The problem is to a large extent complicated due to the lack of an accomplished theory of the high  $T_c$  superconductivity. The modified two fluid empirical model proposed by Vendik et al largely portraits many of the macroscopic properties but fails to explain the vortex effects of high temperature superconductors. As the temperature and the magnetic field are gradually increased, the high  $T_c$  superconducting materials will be in a mixed state. It is observed that the rf conductivity and surface impedance of these type 2 superconducting materials widely vary with

temperature and magnetic field. The microwave losses induced by the static magnetic fields and the varying temperatures have been investigated by many authors. One needs to take into account the combined effects of the applied static magnetic field, the field produced by the microwave radiation and the added field effects due to the moving vortices to analyze the propagation characteristics. The phenomenological unified theory proposed by Coffey and Clem takes care of the vortex dynamics including both the influence of vortex pinning and flux creep in a self consistent manner. Such an approach is extremely

important when we investigate the propagation characteristics to study the efficiency of the microstrip line, where the temperature and applied magnetic fields widely vary. Here we have studied the propagation characteristics of a superconducting microstrip line in mixed state.

## II. TRANSMISSION PROBLEM

We consider radiation normally incident on successive layers of superconducting and non superconducting materials. As shown in fig.1, a slab of superconductor is taken to have a thickness  $d$  while the substrate has a thickness  $t$ . Radiation incident along the X axis encounter the Type 2 superconductor of thickness  $d$  and substrate of thickness  $t$ . All rf magnetic fields are assumed to be in the +Z direction. Within the superconductor the complex penetration depth is  $\tilde{\lambda}$ , within in the substrate the complex wave number is  $\tilde{k}$  and the free space wave vector is  $k_0$ . Consider the substrate to be characterized by a complex index of refraction  $\tilde{n}(\omega, T)$ . We expect to encounter very low loss substrates so that  $\text{Re}(\tilde{n})$  is very much greater than  $\text{Im}(\tilde{n})$  will hold.

It can be seen that the Type 2 superconductor can be considered to be characterized by an effective complex index of refraction

$$\tilde{n}(\omega, B, T) = \frac{i}{k_0 \tilde{\lambda}(\omega, B, T)} \quad (1)$$

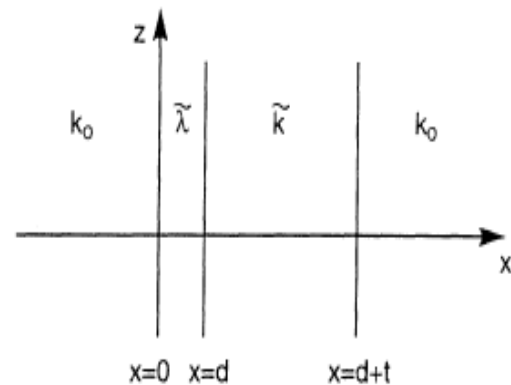


Figure 1: Set up of the transmission problem.

Radiation incident along the X-axis encounters a type-2 superconductor of thickness  $d$  and a substrate of thickness  $t$ . All rf magnetic fields are taken to be in the +Z direction. Within the superconductor the complex penetration depth is  $\tilde{\lambda}$ , within the substrate the complex wave number is  $\tilde{k}$  and the free space wave number is  $k_0$ .

where  $k_0 = \frac{\omega}{c}$  is the free wave number. Let  $\omega$  be the angular frequency of incident radiation and wave number in substrate is  $\tilde{k} = k_0 \tilde{n}$ . For this purpose a static magnetic field of magnitude  $B \geq 2B_{c1}$  will be considered to be applied in the X-Z plane but at an arbitrary angle  $\alpha$  with respect to the x axis. The same expression for complex penetration depth  $\tilde{\lambda}$  holds for all angles  $\alpha$ . For an oblique applied static field for attenuation dominated problems the rf field must be resolved in to two components which decay with different penetration depths. In general, two independent angles are required to describe the superconductor response. The self consistently determined penetration depth  $\tilde{\lambda} = \tilde{\lambda}(\omega, B, T)$  is given in terms of normal fluid skin depth  $\delta_{nf}$  and complex effective skin depth  $\delta_{vc}$  due to vortex motion and creep as

$$\tilde{\lambda}(\omega, B, T) = \sqrt{\frac{\lambda^2 - (j/2)\delta_{vc}^2}{1 + 2j\lambda^2\delta_{nf}^{-2}}} \quad (2)$$

Equation (2) effectively furnishes the dispersion relation of the superconductor. At GHz frequencies we ignore the effect of displacement current in the superconductor which would modify equation (2). The squares of lengths associated with normal fluid and vortex responses, respectively are given in terms of the corresponding resistivities by,

$$\delta_{nf}^2(\omega, B, T) = \frac{2\rho_{nf}}{\mu_0\omega} \quad (3)$$

where  $\rho_{nf}$  is the normal fluid resistivity expressed in terms of the normal state resistivity  $\rho_n$ , as

$$\rho_{nf} = \frac{\rho_n}{f(T, B)} \quad (4)$$

Where

$$f(T, B) = 1 - \left[ 1 - \left( \frac{T}{T_c} \right)^4 \right] \left[ 1 - \frac{B}{B_{c2}(T)} \right] \quad (5)$$

$$\tilde{\delta}_{vc}^2(\omega, B, T) = \frac{2\tilde{\rho}_v}{\mu_0\omega} \quad (6)$$

where  $\tilde{\rho}_v = B\phi_0\tilde{\mu}_v(\omega, b, T)$  and  $\tilde{\mu}_v$  is the complex dynamics vortex mobility given by,

$$\tilde{\mu}_v(\omega, B, T) = \frac{1}{\eta} \left[ 1 + \left[ \frac{j\omega\eta}{\zeta k_p} + \frac{1}{I_0^2(\omega) - 1} \right]^{-1} \right]^{-1} \quad (7)$$

where  $\eta$  is the viscous drag coefficient defined by

$$\eta = \frac{B\phi_0}{\rho_f} \quad (8)$$

where

$$\rho_f = \frac{\rho_n B}{B_{c2}(T)} \quad (9)$$

is the Bardeen-Stephen flux flow resistivity. The force constant of the pinning Potential is given by,

$$k_p = k_{p0} [1 - (T/T_{c2})^2]^2 \quad (10)$$

Where  $T_{c2}$  is the temperature at which  $B = B_{c2}(T)$ . In addition,  $\zeta = \frac{I_1(w)}{I_0(w)}$  where  $I_1$  and  $I_0$  are the modified Bessel functions of first kind of order one and zero respectively, and the argument is defined by,

$$w = \frac{U_0(B, T)}{2K_B T} \quad (11)$$

where the temperature and field dependent barrier height of the periodic potential is given by

$$U_0(B, T) = U \left[ 1 - \left( \frac{T}{T_{c2}} \right) \right]^{3/2} B^{-1} \quad (12)$$

For the above geometry, all rf electric field and current densities are along the  $\pm y$  direction. We assume a common factor  $\exp(-i\omega t)$  for the time dependence of the electrodynamic fields, omitting here a detailed specification of the form of the electric and magnetic fields in each region along the x axis. As usual, electric field amplitudes can be eliminated in favor of magnetic field ones by means of Faraday's law. The remaining magnetic-field coefficients can be found in terms of the incident magnetic-field amplitude  $h_i = b_i/\mu_0$  by enforcing the continuity of the tangential components of the electric and magnetic fields at the three interfaces. These conditions lead to three  $2 \times 2$  matrix equations for the magnetic-field amplitudes, wherein the propagation matrices can be used to determine the wave amplitudes in any region in terms of those of any other region. In writing the final results we introduce the convenient abbreviations

$$e = \cosh(d/\tilde{\lambda}), \quad \mathcal{S} = \sinh(d/\tilde{\lambda}), \quad \epsilon_{\pm}^t = \exp(\pm i\tilde{k}t) \quad (13)$$

The algebraic solution of the coupled matrix equations gives the transmission coefficient  $T = |b_t|^2/|b_i|^2$  as

$$T = \frac{16|\tilde{k}|^2|\tilde{\lambda}|^2}{D} \quad (14)$$

Where the denominator is

$$D = |\epsilon^t - (1 + \tilde{k}/k_0)[\mathcal{S}(1 - \tilde{k}k_0\tilde{\lambda}^2) - i(\tilde{k} + k_0)\tilde{\lambda}e] - \epsilon_+^t(1 - \tilde{k}/k_0)[\mathcal{S}(1 + \tilde{k}k_0\tilde{\lambda}^2) + i(\tilde{k} - k_0)\tilde{\lambda}e]|^2 \quad (15)$$

Similarly, the reflection coefficient

$$R = |b_r|^2 / |b_i|^2$$

$$R = \left| \epsilon_{\pm}^t (1 + \tilde{k}/k_0) [sS(1 + \tilde{k}k_0\tilde{\lambda}^2) - i(\tilde{k} - k_0)\tilde{\lambda}e] - \epsilon_{\pm}^t (1 - \tilde{k}/k_0\tilde{\lambda}^2) + i(\tilde{k} + k_0)\tilde{\lambda}e \right|^2 / D. \quad (16)$$

Equations (16) give the expected expressions when either the superconductor is absent ( $d \rightarrow 0, sS \rightarrow 0, e \rightarrow 1$ ) or the substrate is absent ( $t \rightarrow 0, \epsilon_{\pm}^t \rightarrow 1, \tilde{k} \rightarrow k_0$ ). The T and R coefficients for layered media can be calculated from successive inversions of propagation matrices.

### III. NUMERICAL ANALYSIS

We have studied a phenomenological theory for microwave characteristics of high temperature superconducting thin films. The theory includes the effects of vortex inertia, pinning, flux flow and flux creep in a unified manner by using complex dynamic vortex mobility. Here we compare the transmission and reflection coefficient of high temperature superconducting films with the value of the parameter  $\gamma=4$  and  $\gamma=2$ .

#### A. London penetration depths as a function of temperature

The dependence of penetration depth  $\lambda_L(T)$  of a magnetic field in high-Tc superconductors can be generally approximated in the binomial form as

$$[\lambda_L(0)/\lambda_L(T)]^2 = 1 - (T/T_c)^\gamma$$

where  $\lambda_L(0)$  is the penetration depth for  $T \rightarrow 0$ .

The simplest theoretical model of high-Tc superconductors yields  $\gamma = 1.5$ . More rigorous study of the nature of high-Tc superconductors yields a dependence of  $\lambda_L(T)$  similar to that given by the Bardeen-Cooper-Schrieffer (BCS) theory. Most of the theoretical studies based on a concept of gap features in high-Tc superconducting materials - two gaps, gaps with nodes, gapless model or on the inhomogeneity or multiphase nature of the composition of high-Tc superconductors, arrive at the idea of description of the dependence  $\lambda_L(T)$  in the form given by above equation. The parameters  $\lambda_L(0)$  and  $T_c$  can be determined based on experimental data. By the analysis the parameters are obtained as  $T_c = 7.198$  K,  $\lambda_L(0) = 48.1$  nm,  $\gamma = 0.06$  which are in very good agreement with the commonly used Gorter-Casimir presentation for the low temperature superconductors. The experimental results can be obtained for Y-Ba-Cu-O superconductors. The Y-Ba-Cu-O films may be classified into two groups: high-quality films  $\lambda_L(0) \leq 150$  nm,  $T_c \geq 89$  K and low-quality films  $\lambda_L(0)$  greater than 150 nm,  $T_c$  less than 89K. Based on the experimental data it may be concluded that a phenomenological description of  $\lambda_L(T)$  for high quality Y-Ba-Cu-O films may be achieved for  $\gamma = 2.0$ . For low quality films,  $\gamma = 1.5$  is more accurate. Among some experimental results, one may find  $\gamma = 1.3 - 1.4$ . The smoother dependence of  $\lambda_L(T)$  for low quality films may be attributed to the broadening of the phase transition caused by inhomogeneity of the phase

composition of the films. Thus, the Gorter-Casimir relations can be applied to the low temperature superconductors with  $\gamma = 4:0$  and to the HTS's with  $\gamma = 1.3 - 2.1$ . The two-fluid model applied to HTS's is called the "enhanced" two-fluid model.

#### B. Theoretical formulation

For conventional superconductors such as Pb, Sn and Nb which were known in the time when Gorter and Casimir model had been suggested, a good agreement with the experiment was obtained by  $\gamma = 4$ . Since  $n_s(T)$  is closely connected with  $\lambda_L(T)$ , the penetration depth of a magnetic field by the equation,

$$\frac{1}{\lambda_L(T)^2} = \frac{e^2 n_s(T) \mu_0}{m_s}$$

Where  $e$  and  $m_s$  are charge and effective mass of an electron and  $\mu_0$  is the free space magnetic permeability. Thus from the above equation we can see that as  $n_s(T)$  increases  $\lambda_L(T)$  decreases. We know,

$$\frac{1}{\lambda_L(T)^2} = \frac{e^2 n_s(0) \mu_0}{m_s}$$

Dividing these we get,

$$\lambda_L(T) = \frac{\lambda_L(0)}{\sqrt{1 - (T/T_c)^\gamma}}$$

Where  $\lambda_L(0)$  is the penetration depth at  $T = 0$  K. Based on the above theory we have performed numerical computations. Here we are studying about high quality films with  $T_c = 92$  K. While Coffey-Clem proposed the model, the accurate value of  $\gamma$  was 4. But the study of Vendik et al has now been accepted widely where the value of  $\gamma$  is made to vary from 1.5 to 3.0. We take  $\gamma = 2$  in our study and compare it with  $\gamma = 4$  for various applications. If we take  $\gamma = 2$  we get

$$\lambda_L(T) = \frac{\lambda_L(0)}{\sqrt{1 - \left(\frac{T}{T_c}\right)^2}}$$

$$f(T, B) = 1 - \left[1 - \left(\frac{T}{T_c}\right)^2\right] \left[1 - \frac{B}{B_{c2}(T)}\right]$$

If we take  $\gamma = 2$ , due to the changes in  $\lambda_L(T)$  and  $f(T, B)$  there are changes in conductivity.

The numerical results serve to illustrate the temperature and field dependence of quantities such as the reflection and transmission coefficients. In the following  $t = T/T_c$  denotes the reduced temperature and  $b = B/B_{c2}(0)$  denotes the reduced field. All numerical result to follow 0.5mm for substrate thickness and  $\tilde{n} = 4 + i10^{-4}$  for its complex index of refraction,  $2100A^0$  for the superconductor thickness, 33GHz as the frequency of applied radiation. The material parameters used are the typical values of high Tc superconducting system of YBCO.  $\rho_n(T) = 1.1 \times 10^{-8} T + 2 \times 10^{-6} \Omega m$ ,  $U = 0.15$  eV,  $K_{p0} = 2.1 \times 10^4$  N/m and  $B_{c2} = 112$  T,  $\varphi_0 = h/2e = 2.0678 \times 10^{-15} T m^2$ .

IV. NUMERICAL RESULTS AND DISCUSSIONS

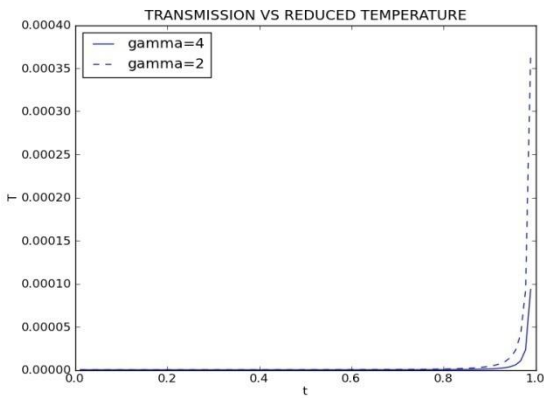


FIG.1.The transmission coefficient is plotted versus the reduced temperature (t) at 33 GHz for reduced field b=0 for gamma=4 and gamma=2.

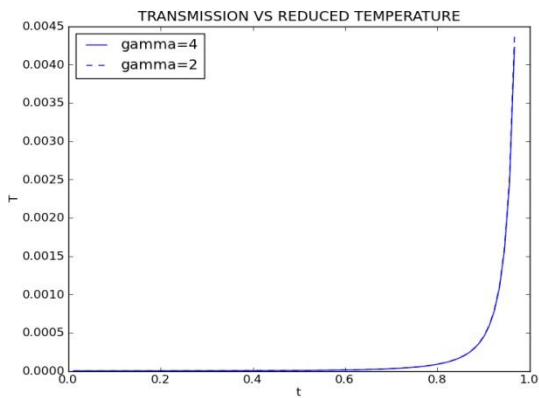


FIG.2.The transmission coefficient is plotted versus the reduced temperature (t) at 33 GHz for reduced field b=0.025 for gamma=4 and 2.

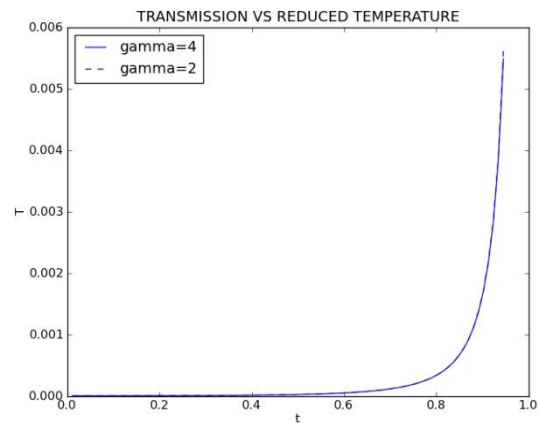


FIG.3.The transmission coefficient is plotted versus the reduced temperature (t) at 33 GHz for reduced field b=0.05 for gamma=4 and 2.

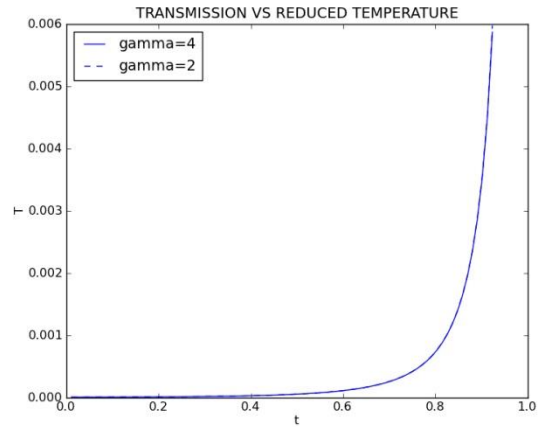


FIG.4.The transmission coefficient is plotted versus the reduced temperature (t) at 33 GHz for reduced field b=0.075 for gamma=4 and 2

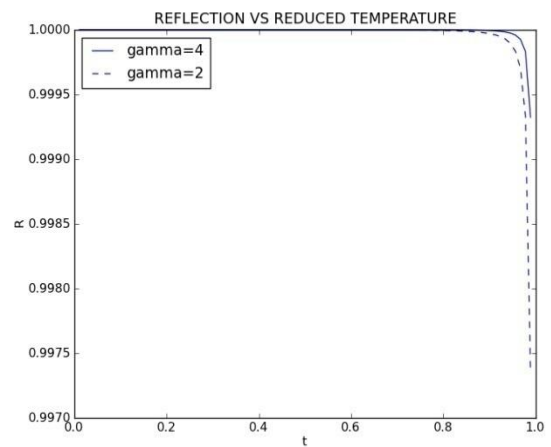


FIG.5.The reflection coefficient is plotted versus the reduced temperature (t) at 33 GHz for reduced field b=0 for gamma=4 and gamma=2.

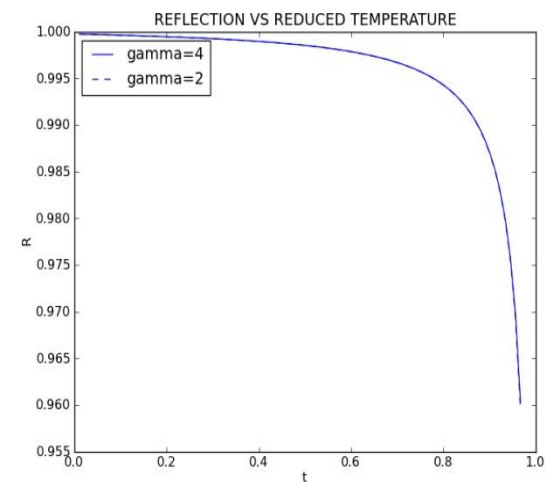


FIG.6.The reflection coefficient is plotted versus the reduced temperature (t) at 33 GHz for reduced field b=0.025 for gamma=4 and gamma=2.

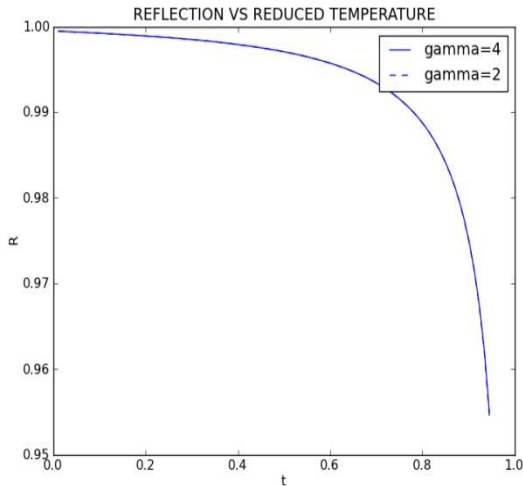


FIG.7.The reflection coefficient is plotted versus the reduced temperature (t) at 33 GHz for reduced field  $b=0.05$  for  $\gamma=4$  and  $\gamma=2$ .

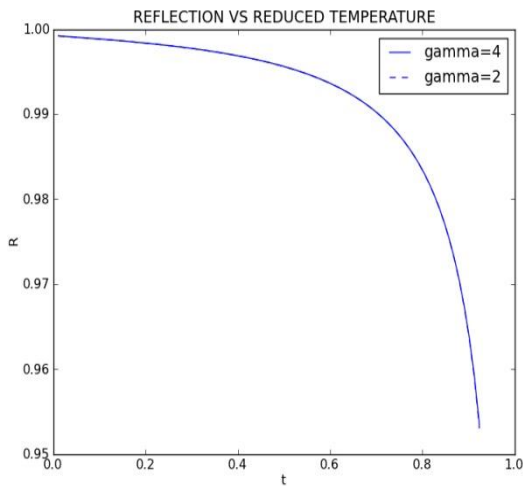


FIG.8.The reflection coefficient is plotted versus the reduced temperature (t) at 33 GHz for reduced field  $b=0.075$  for  $\gamma=4$  and  $\gamma=2$ .

Fromfig.1 to fig.8 the transmission and reflection coefficient versus reduced temperature for different values of the applied static field  $b=0, 0.025, 0.05, 0.075$  at 33 GHz. The transmission coefficient  $T$  exhibit a step like rise as a function of temperature which broadens with increasing field, reaching a normal state value at  $T_{c2}$ . The reflection coefficient decreases near the field dependent transition temperature  $T_{c2}$ . Transmission coefficient for  $\gamma = 2$  and  $\gamma = 4$  are plotted versus reduced temperature  $t$  at constant reduced static field  $b=0, 0.025, 0.05, 0.075$ . From the graphs we can see that the value of  $T$  increases gradually as the reduced temperature increases and  $R$  decreases as reduced temperature increases. Here we can see that there is only a very small variation in  $T$  and  $R$  when we replace the value of  $\gamma = 4$  by  $\gamma = 2$ . The change between values of  $\gamma = 4$  and  $\gamma = 2$  for  $R$  and  $T$  is only considered at very high temperature.

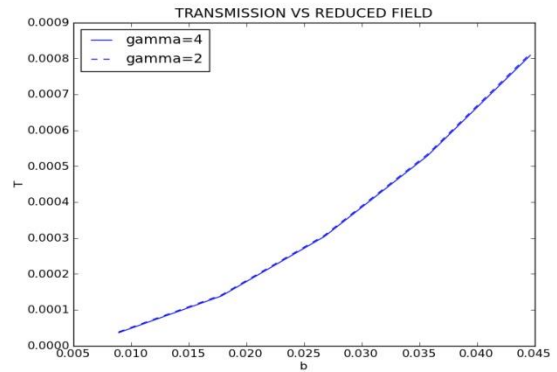


FIG.9.The transmission coefficient is plotted versus the reduced field (b) at 33 GHz for reduced temperature  $t=0.875$  for  $\gamma=4$  &  $\gamma=2$

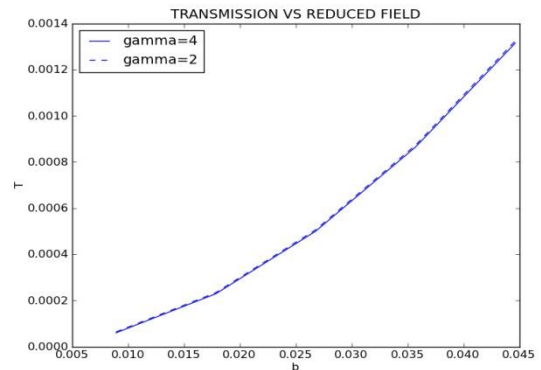


FIG.10.The transmission coefficient is plotted versus the reduced field (b) at 33 GHz for reduced temperature  $t=0.90$  for  $\gamma=4$  and  $\gamma=2$ .

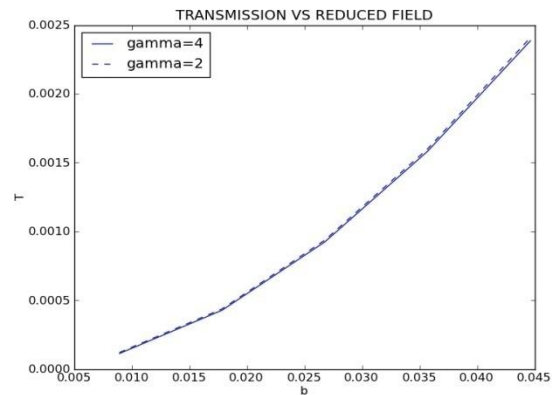


FIG.11. the transmission coefficient is plotted versus the reduced field (b) at 33 GHz for reduced temperature  $t=0.925$  for  $\gamma=4$  and  $\gamma=2$ .

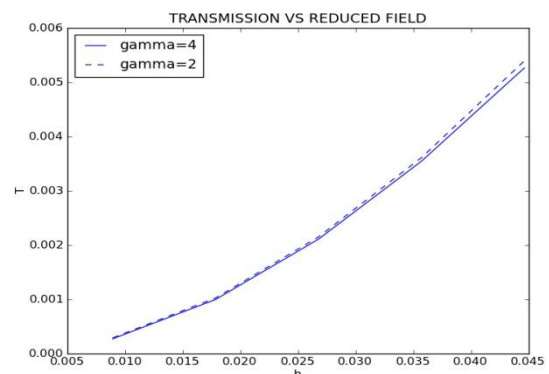


FIG.12.The transmission coefficient is plotted versus the reduced field (b) at 33 GHz for reduced temperature  $t=0.95$  for  $\gamma=4$  and  $\gamma=2$ .



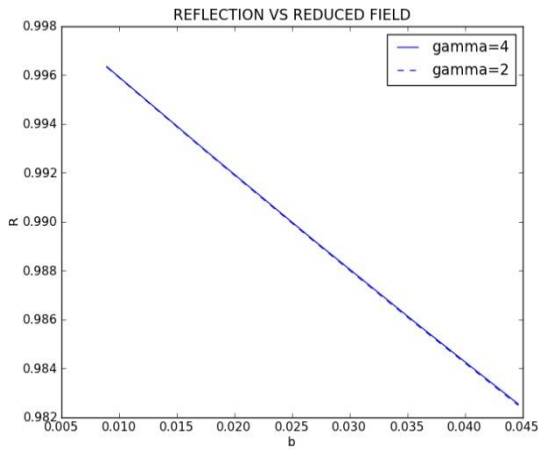


FIG.13.The reflection coefficient is plotted versus the reduced field (b) at 33 GHz for reduced temperature  $t=0.875$  for  $\gamma=4$  and  $\gamma=2$ .

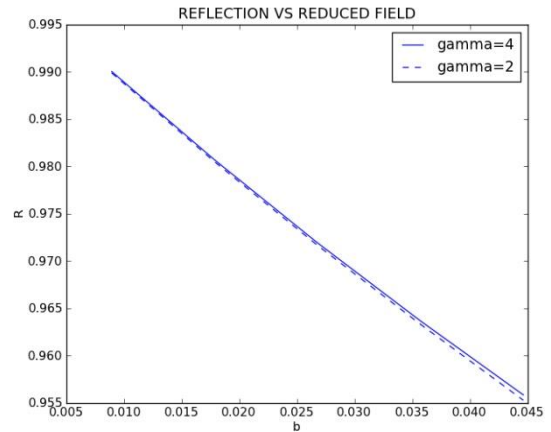


FIG.16.The reflection coefficient is plotted versus the reduced field (b) at 33 GHz for reduced temperature  $t=0.95$  for  $\gamma=4$  and  $\gamma=2$ .

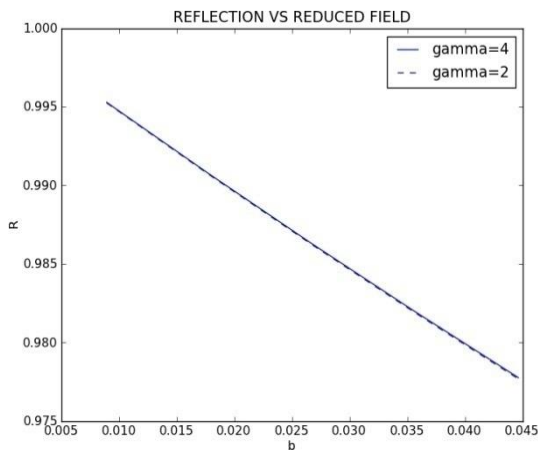


FIG.14.The reflection coefficient is plotted versus the reduced field (b) at 33 GHz for reduced temperature  $t=0.90$  for  $\gamma=4$  and  $\gamma=2$ .

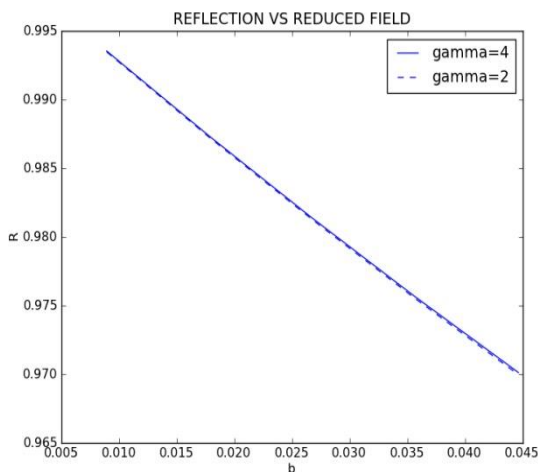


FIG.15.The reflection coefficient is plotted versus the reduced field (b) at 33 GHz for reduced temperature  $t=0.925$  for  $\gamma=4$  and  $\gamma=2$ .

From fig.9 to fig.16 the transmission and reflection coefficient versus reduced fields for different values of the temperature  $t=0.875, 0.90, 0.925, 0.95$  at 33 GHz. The transmission coefficient  $T$  exhibits a linear rise as a function of temperature with increasing reduced field. The reflection coefficient exhibits a linear decrease with increasing reduced field. Transmission coefficient for  $\gamma = 2$  and  $\gamma = 4$  are plotted versus reduced temperature  $t$  at constant reduced static field  $b=0, 0.025, 0.05, 0.075$ . From the graphs we can see that the value of  $T$  increases gradually as the reduced temperature increases and  $R$  decreases as reduced temperature increases. Here we can see that there is only a very small variation in  $T$  and  $R$  when we replace the value of  $\gamma = 4$  by  $\gamma = 2$ . The change between values of  $\gamma = 4$  and  $\gamma = 2$  for  $R$  and  $T$  is observed at high reduced field.

### V. CONCLUSION

Based on the studies of high  $T_C$  superconductor the transmission and reflection of superconducting films is calculated using Coffey-Clem model. The values of transmission and reflection coefficient are plotted for the values of  $\gamma=2$  and  $\gamma=4$ , where  $\gamma$  is a parameter based on which the complex penetration depth of the type 2 superconductor varies.

The values of the transmission and reflection coefficient are plotted with the parameter  $\gamma=2$  and  $\gamma=4$ . Numerical results demonstrate that the transmission and reflection coefficient has no appreciable change for  $\gamma=2$  and  $\gamma=4$ , when the temperature is fixed. But at very high temperature the value of  $R$  and  $T$  is found to slightly vary for  $\gamma=2$  and  $\gamma=4$ . So when experiments are conducted at very high reduced temperature the value of  $\gamma$  should be correctly used in determining  $R$  and  $T$ . But when we plot the transmission and reflection coefficient versus reduced field a slight variation observed. This variation increases as the reduced temperature increases.

## ACKNOWLEDGEMENT

I owe my deepest gratitude to my guide Fr. Jolly Andrews, Assistant Professor, Department of Physics, Christ College, Irinjalakuda, for his valuable guidance, encouragement and his constant support throughout work.

## REFERENCES

- [1] C. Song, M. P. Defeo, K. Yu, B. L. T. Plourde, Appl. Phys. Lett. 95 (2009) 232 501.10
- [2] K. Matsumoto, P. Mele, Supercond. Sci. Technol. 23 (2010) 14 001.
- [3] A. A. Gallitto, S. Fricano, M. L. Vigni, Phys. C 384 (2003) 11.
- [4] M. Tinkham, Introduction to Superconductivity, Dover Books on Physics, (2004).
- [5] M. W. Coffey and J.R. Clem, IEEE Trans. Magn. 27, 2136(1991); 27, 4396(E)1991
- [6] O. G. Vendik, I. B. Vendik, D. I. Kaparkov, IEEE Trans. MTT 46 (1998) 469.
- [7] Y. Kobayashi and T. Imai, ICICE Trans. Electronics, E74-C, (1991) 1986.
- [8] J. G. Ma, I. Wolff, IEEE Trans. MTT 43 (5) (1995) 1053.
- [9] J. G. Ma, I. Wolff, IEEE Trans. MTT 44 (4) (1996) 537.
- [10] C. P. Poole, Handbook of Superconductivity, Academic Press (2000)
- [11] A. Heinrich, M. Kuhn, B. Schey, W. Beigel, B. Stritzker, Physica C, 405(2004)